Structural Chemistry (2022) 33:649–669
https://doi.org/10.1007/s11224-022-01878-3

ORIGINAL RESEARCH

# Multi-targeted molecular docking, drug-likeness and ADMET studies of derivatives of few quinoline- and acridine-based FDA-approved drugs for anti-breast cancer activity

**Lai Cong Sing[1] · Anitha Roy[2] · Lok Yong Hui[1] · Chan Sook Mun[1] · Harish Rajak[3] · Rohini Karunakaran[4,5] · Veerasamy Ravichandran[1,5,6]**

Received: 15 November 2021 / Accepted: 6 January 2022 / Published online: 19 January 2022


## Abstract

Quinoline- and acridine-based drugs are widely used as anti-breast cancer agents. These drugs act through various mechanisms of action; for example, neratinib acts on epidermal growth factor receptor 1 (EGFR) and human epidermal receptor type 2 (HER2) enzymes, whereas amsacrine and pyrazoloacridine act on topoisomerase II enzymes. The objective of the present study was to explore and compare the interaction mechanism of knowledge-based designed derivatives of FDA-approved quinoline- and acridine-based drugs. The above-stated cancer proteins were collected from PDB, prepared by correcting any broken chains, removing water and adding charges. Docking studies were performed in the PyRx docking tool, and Discovery Studio Visualizer was used to visualize the molecular interactions. The result obtained found that neratinib had a better binding affinity towards EGFR and HER2 but weaker binding affinity towards topoisomerase IIα and topoisomerase IIβ. On the other hand, amsacrine and pyrazoloacridine were found to have better binding scores in topoisomerase IIα and topoisomerase IIβ instead of EGFR and HER2, as already proved experimentally. All the designed molecules have shown better binding affinity to their favourable enzymes and other enzymes involved in breast cancer development. The outcome reveals that the designed quinoline- and acridine-based drugs derivatives could be examined as a potent inhibitory drug of breast cancer for their strong multi-targeted inhibition ability and reactivity. Further synthesis, in vitro and in vivo investigations of designed derivatives may be done to prove their therapeutic potential in breast cancer treatment.

**Keywords** Quinoline · Acridine · Molecular Docking · EGFR and HER2 · Topoisomerase · Breast Cancer

## Introduction

Cancer is commonly depicted as a chronic abnormal cell disorder in which the ab-normal cell is growing uncontrollably. With its unrestricted cell proliferation, it can be invasive, metastatic and continuously spread to different parts of our body and affect the organs' functions. Breast cancer is one of the most aggressive malignant tumours in women. The statistic obtained in GLOBACAN 2020 found that breast cancer represents 1 in the four cancers diagnosed in women globally [1].

As males and females have identical breast tissues, breast cancer also occurs in males. According to research done by Siegel et al. (2020), the estimated number of breast cancer new cases in the year 2020 of the USA is 279,100 people (2620 male and 276480 female) [2]. About 15% of the total cancer deaths of women were due to breast cancer, which was around 630 thousand women around the

**Highlights**
- Selected target proteins were EGFR, HER2, Topoisomerase IIα, Topoisomerase IIβ.
- Two of the designed molecules have shown better binding affinity.
- All the designed molecules have shown same pharmacokinetic properties as parent drug.
- All the quinoline and acridine derivatives were recognised as drug-like with passing Lipinski's rule of 5.
- There was a big difference in the binding affinities of known drugs and the designed derivatives indicate that the designed molecule could be considered for treatment of breast cancer.

✉ Veerasamy Ravichandran
phravi75@rediffmail.com; ravichandran_v@aimst.edu.my

Extended author information available on the last page of the article

world each year [3]. According to the American Cancer Society, in the USA, one out of eight women is diagnosed with breast cancer in their lifetime. The American Cancer Society Cancer Action network states that black women are 40% more likely to die from breast cancer than white women. Every 13 min. a woman loses her life due to breast cancer [4]. It has been estimated that the worldwide incidence of women breast cancer will reach around 3.2 million new cases annually in 2050 [5]. Thus, it is essential to find effective preventive and treatment measures as the number showed the huge magnitude of breast cancer incidence. Although advances in technology in health care and medical sciences made early detection of the disease possible, treatment can be started as soon as diagnosed. However, there are many unanswered questions regarding the molecular mechanisms that underline certain forms of this cancer [6].

The epidermal growth factor receptor (EGFR) family contains transmembrane tyrosine kinases: HER1, HER2, HER3 and HER4 (also known as ERBB1, ERBB2, ERBB3 and ERBB4, respectively). EGFR overexpression is widely observed in breast cancer. EGFR overexpression determines abnormal regulation of the cells natural function (e.g. cell proliferation, differentiation and survival). Overexpression of EGFR causes strong stimulation of downstream signalling pathways responsible for inducing cell growth, cell differentiation, cell motility, apoptosis and cell cycle progression [7]. Thus, EGFR inhibition is a rational approach for developing anti-breast cancer therapies [8].

DNA encodes important genetic information, and it plays an important role in maintaining cellular function such as replication, encoding information, gene expression, recombination and mutation. Therefore, topological properties of DNA, such as under-winding and overwinding, tangling, knotting, are essential as the topological properties influence major nucleic processes [9]. DNA topoisomerase is an enzyme that alters the topological properties of the DNA By formation of transient single-stranded (topoisomerase I) or double-stranded (topoisomerase II); topoisomerase releases the helical tension from the unwinding of DNA helix because of replication and transcription of DNA.

In human cells, there are a total of six genes encoding six topoisomerases (topoisomerase I, mitochondrial topoisomerase I, topoisomerase IIα, topoisomerase IIβ, topoisomerase IIIα and topoisomerase IIIβ). In this research study, we only focus on topoisomerase II as the target binding protein. There are two forms of topoisomerase II: topoisomerase IIα and topoisomerase IIβ. Topoisomerase IIα acts as a biomarker for cell proliferation as it is overexpressed in proliferating cells, whereas topoisomerase IIβ is evenly distributed in all cells. Topoisomerase IIα and topoisomerase IIβ are 70% identical in amino acid sequences. However, they are encoded in humans by genes on different chromosomes. Topoisomerase IIα and topoisomerase IIβ are encoded by genes on chromosomes 17 and 3, respectively [10]. The topoisomerase II activity recognises and binds the first double-stranded DNA chain (G-segment) on the DNA gate and then the second double-stranded DNA chain (T-segment) at the N-terminal domain through ATPase domain dimerization. A covalent complex formed between DNA and topoisomerase II after the cleavage of G-segment. After that, T-segment will pass through the transient break of the G-segment, mediated through ATP hydrolysis. Then, relegation of G-segment occurs, the C-gate and N-gate open, and G-segment and T-segment are released [11]. As topoisomerase II activities are heavily related to the topological changes in DNA, which affects the process of cell proliferation, the inhibition of topoisomerase II has become an effective strategy in breast cancer therapy, especially topoisomerase IIα inhibition as topoisomerase IIα overexpression contributes to cancer cell proliferation [12]. Hence, EGFR, HER2 and topoisomerase II were selected for the present *in silico* study than other enzymes and receptors responsible for breast cancer.

Quinoline- and acridine-based drugs are widely used in the pharmaceutical field. The prominent ones include antiviral (e.g. saquinavir), antibacterial (e.g. gatifloxacin, sparfloxacin, fluoroquinolones, ciprofloxacin), anthelmintic (e.g. oxamniquine), antifungal-antiprotozoal (e.g. clioquinol), anti-malarial (e.g. quinidine, quinine, chloroquine, mefloquine, primaquine, amodiaquine, etc.), antituberculosis (e.g. ciprofloxacin, moxifloxacin), local anaesthetic (e.g. dibucaine), antiasthmatic (e.g. montelukast) and antipsychotic (e.g. brexpiprazole aripiprazole) [13]. Examples of quinoline drugs used in cancer treatment are neratinib, pelitinib, dovitinib, tipifamib, quarfloxin and roquinimex, and acridine drugs are amsacrine and pyrazoloacridine. The main hypothesis of the present work was that the designed quinolone- and acridine-based drugs derivative could have same drug-likeness properties as selected drugs and have better molecular interaction with multiple binding sites in breast cancer than the known drugs used in the present study.

Although many drug discoveries to combat breast cancer have been done [9, 14–28], there is no direct treatment or drug that is fully effective or completely cure all types of breast cancer [3]. Many studies have been done on quinoline derivatives in treating breast cancer. The ideal drugs for anti-cancer are that they can act on most of the enzymes involved in breast cancer development. Unfortunately, until today, there are no anti-cancer agents that meet this criterion. To improve the therapeutic potential and expand the scope of drugs, one of the methods used is to design new derivatives from already approved drugs by modifying structural features. This prompted us to carry out the present

multi-targeted molecular docking study on quinolone- and acridine-based drugs derivatives against different enzymes involved in breast cancer development and predicted molecular interactions. The outcome of the present study reveals that the modified drug structures possess better binding efficacy towards the target than their parent compounds. Predicted ADMET studies of all these compounds indicate lipophilic, low gastrointestine absorbable and no blood–brain barrier permeable properties.

## Materials and Methods

The structure of chemical compounds (NRT, AMS and PZA) was collected from the online database Pubchem, and 3D structures of breast cancer enzymes (EGFR, HER2, topoisomerase IIα and topoisomerase IIβ) were collected from Protein Data Bank. The modelling software such as Chem Office-16 (http://www.cambridgesoft.com/Ensemble_for_Chemistry/details/Default.aspx?fid=16), Discovery Studio Visualizer 3.0 (https:// discover.3ds.com/discovery-studio-visualizer-download), Swiss Protein Data Base Viewer (https://spdbv.vital-it.ch/), Open Babel (http://openbabel.org/wiki/Main_Page), PyRx (https://pyrx.sourceforge.io/), and AutoDock Vina (http://vina.scripps.edu/) was used in the present study. Online tools such as Swiss ADME (http://www.swissadme.ch/) and ProTox-II (https://tox-new.charite.de/protox_II/index.php?site=compound_search_similarity) were also used.

### Preparation of Ligands

The structure of the NRT, AMS and PZA was downloaded from PubChem, and designed derivatives (NRT1, AMS1 and PZA1) (Fig. 1) were drawn using the Chem Draw tool of Chem Office-16 and then saved as either a .sdf or .mol file for further use. Then, the structures were checked for ADMET and Lipinski rule of five by using online tools SwissADME and ProTox-II.

### Preparation of Proteins

The crystallographic structure of enzymes of breast cancer, which were EGFR (Fig. 2A), HER2 (Fig. 2B), topoisomerase IIα (Fig. 2C) and topoisomerase IIβ (Fig. 2D), was downloaded from Protein Data Bank (PDB) and checked for any broken chain or any other missed atoms or chain in the structure using Swiss Protein Data Base Viewer and corrected. The information about the enzyme's active site was retrieved from PDB, gathered from related published articles, or found out by using Discovery Studio Visualizer. Then, water and other heteroatoms were removed from the structure of the protein, and the protein structures were saved in PDB format [29].

### Docking Studies

The compounds and protein/enzyme structures were uploaded in the docking tool PyRx. The selected chemical compounds were imported into Open Babel within the Python Prescription Virtual Screening Tool (PyRx) and subjected to energy minimization. The energy minimization was performed with the Universal Force Field (UFF) using the conjugate gradient algorithm. The total number of steps was set to 200, and the number of steps for update set to 1. In addition, the minimization was set to stop at an energy difference of less than 0.1 kcal/mol. After energy minimization, both chemical compounds and protein/enzyme structure were saved as '.pdbqt' format using the Open Babel tool in PyRx. When the compounds converted to '.pdbqt' format in Open Babel within PyRx, the charges can be automatically added to generate ligand atomic coordinates for docking. PyRx is using PyBabel charges, by default. Then, the active binding site grid box was generated for the enzymes by using PyRx [29]. The docking simulation was run at an exhaustiveness of 8 and set to only output the lowest 9 energy poses. The conformational search algorithm used in PyRx is Lamarckian genetic algorithm. The docking output files were analysed for the interactions between the chemical compounds with the amino acid of protein using Discovery Studio Visualizer [30]. First, the validation and evaluation of the docking protocol were performed by re-docking the ligand extracted from the crystallographic structure of the protein using the PyRx tool. The root means square deviation (RMSD) for the extracted ligand conformations was below 2 Å when compared to the crystallographic form of the ligand [31].

After docking, the docking or binding score was saved in '.csv' format. Autodock Vina was used to separating complex conformers into an individual one. Then, the docking output files were analysed by Discovery Studio Visualizer to find the interactions between the chemical compounds with an amino acid of the protein. The best conformer was selected based on the docking score and better non-covalent hydrogen bond interaction. The pictures of the docking pose and interactions were collected and saved [30].

## Results and Discussion

The present research work evaluated the known quinoline and acridine drugs, and their designed derivatives for drug-likeness and ADME (absorption, distribution, metabolism and excretion) analysis through the SwissADME online

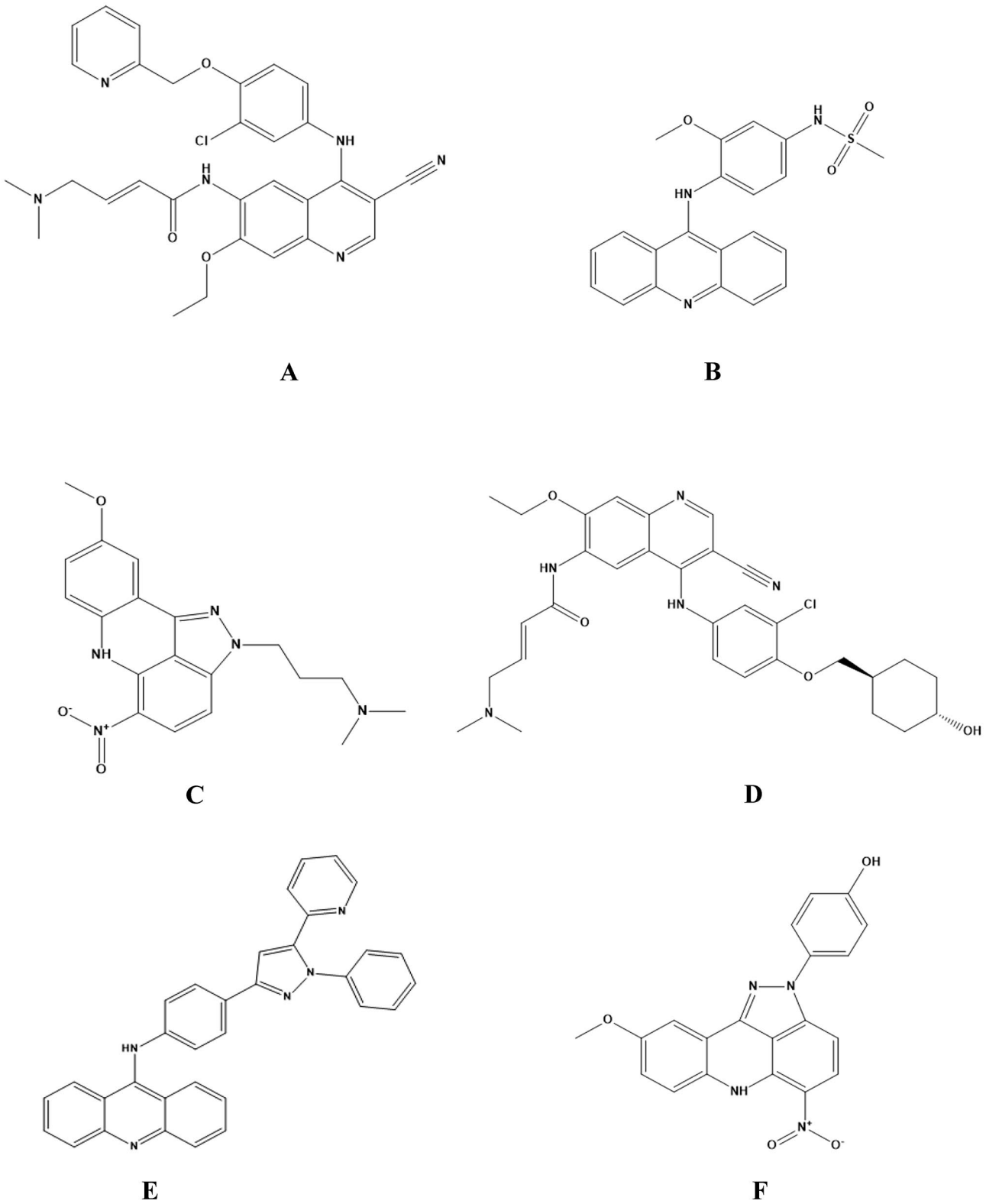


**Fig. 1** Structure of **A**) neratinib (NRT), **B**) amsacrine (AMS), **C**) pyrazoloacridine (PZA), **D**) NRT1, **E**) AMS1, **F**) PZA1

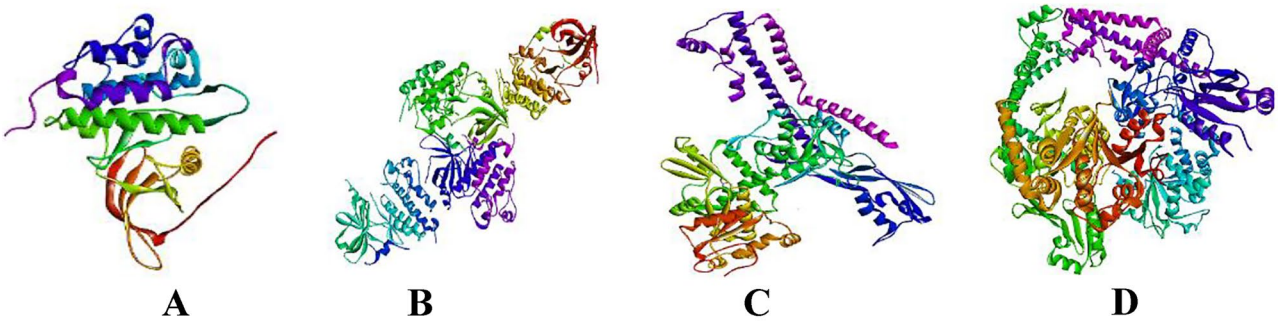


**Fig. 2** Structure of breast cancer proteins **A**) EGFR (PDB ID: 1M17); **B**) HER2 (PDB ID: 3RCD); **C**) topoisomerase IIα (PDB ID: 4FM9); **D**) topoisomerase IIβ (PDB ID: 4G0V)

tool and toxicity prediction by ProTox-II. The results are shown in Table 1. The drug-likeness and ADMET of known drugs were calculated for comparison. From Table 1, it is seen that all designed derivatives were found to have suitable ADMET values compared to known drugs and fulfilled the drug-likeness properties, except both NRT and NRT1 with a molecular weight of >500 g/mol, and NRT, AMS, NRT1 and AMS1 have logP value of >5.0. The predicted molecular weight of AMS1 is 96 g/mol more than AMS. The number of rotatable bonds in PZA1 is just half of the number of rotatable bonds present in PZA. The topological polar surface area values are less than 130. There are not many changes in other drug-likeness properties of the known drugs and their designed derivatives. All the compounds showed no blood brain barrier permeant property with good bioavailability score of 0.55. Except AMS1, all other compounds showed immunotoxicity in online tool prediction. Predicted LD50 of AMS1 and PZA1 is better than their parent drug. The computation prediction of drug-likeness and ADMET properties indicated that the designed derivatives could behave as drug with tolerable pharmacokinetic properties, even though both known and designed derivatives were showing some violation.

Then, docking studies were carried out on known quinolone-based drug neratinib (NRT), and acridine-based drugs amsacrine (AMS) and pyrazoloacridine (PZA) and their derivatives (Fig. 1) to understand their interaction with breast cancer proteins (Fig. 2). The coordinate and distance of the x, y and z axes of the grid boxes of each protein molecule are shown in Table 2, which were determined with

**Table 1** Drug-likeness, pharmacokinetics and ADMET properties of known quinoline- and acridine-based drugs and their derivatives

| Properties | Neratinib (NRT) | Amsacrine (AMS) | Pyrazoloacridine (PZA) | NRT1 | AMS1 | PZA1 |
|---|---|---|---|---|---|---|
| Molecular Weight (g/mol) | 557.05 | 393.46 | 367.40 | 578.11 | 489.57 | 374.35 |
| logP | 5.59 | 5.40 | 3.64 | 5.70 | 5.74 | 4.28 |
| Hydrogen bond acceptor | 2 | 2 | 1 | 3 | 1 | 2 |
| Hydrogen bond donor | 7 | 4 | 5 | 7 | 3 | 5 |
| Rotatable bond | 12 | 5 | 6 | 12 | 5 | 3 |
| Topological Polar surface area (A) | 237.57 | 88.70 | 91.90 | 119.74 | 55.63 | 108.89 |
| GI absorption | Low | High | High | Low | Low | High |
| BBB permeant | No | No | No | No | No | No |
| Bioavailability Score | 0.55 | 0.55 | 0.55 | 0.55 | 0.55 | 0.55 |
| Hepatotoxicity | Inactive | Active | Inactive | Inactive | Active | Active |
| Carcinogenicity | Inactive | Active | Active | Inactive | Active | Active |
| Immunotoxicity | Active | Active | Active | Active | Inactive | Active |
| Cytotoxicity | Inactive | Inactive | Inactive | Inactive | Inactive | Inactive |
| Predicted $LD_{50}$ (mg/kg) | 4000 | 53 | 580 | 1000 | 1400 | 1400 |
| Predicted Toxicity class | 5 | 3 | 4 | 4 | 4 | 4 |

Known quinolone-based drugs: NRT, AMS, PZA, designed quinolone- and acridine-based compounds: NRT1, AMS1, PZA1

**Table 2** Coordinate of the x, y and z centres of grid boxes of breast cancer proteins with dimensions

| Protein molecule | x- centres (dimension) | y-centres (dimension) | z-centre (dimension) |
|---|---|---|---|
| EGFR | 22.08 (25 Å) | 0.26 (25 Å) | 52.77 (25 Å) |
| HER2 | –12.42 (25 Å) | –13.83 (25 Å) | –23.29 (25 Å) |
| Topoisomerase IIα | 17.59 (25 Å) | 39.24 (25 Å) | 25.29 (25 Å) |
| Topoisomerase IIβ | 23.84 (25 Å) | 116.03 (25 Å) | 37.64 (25 Å) |

the help of a Discovery Studio Visualizer, and the same values were used for the docking of the designed compounds. Table 3 shows the binding affinity of the known quinoline base drugs and designed quinoline base compounds with the targets. Table 4 shows the interacted amino acids of breast cancer proteins with the known and designed quinoline base compounds. Table 5 shows the donors and acceptors of compounds and amino acids involved in the formation of hydrogen bond. In majority of the C-H bond interaction, the "carbon" comes from the drug molecule.

NRT, AMS and PZA showed the binding score of -7.7 kcal/mol, -6.9 kcal/mol and -6.4 kcal/mol, respectively, against EGFR. Among all these three ligands, NRT showed the highest affinity towards EGFR than the other two ligands. Figure 3A–C shows the interactions between NRT and EGFR. NRT formed a strong conventional hydrogen bond with Leu694 (1.85Å), one weak carbon-hydrogen bond with Val693 (3.72Å), alkyl interaction with Cys773 (3.97Å) and Arg817 (4.21Å), and a pi-alkyl interaction with Phe699 (3.93Å) of EGFR. AMS formed conventional hydrogen bonds with Lys721 (2.01Å) and Asn818 (2.37Å), pi-anion interaction with Asp831 (3.21Å) and pi-alkyl interaction with Cys773 (4.35Å and 4.93Å) and Arg817 (4.49Å and 4.52Å) of EGFR. Figure 3D–F shows the interactions between AMS and EGFR. PZA formed carbon-hydrogen bonds with Asn818 (3.73Å) and Asp831 (3.33Å), pi-anion interaction with Asp831 (3.95Å and 4.46Å) and a pi-sulphur interaction with Cys773 (5.66Å). Three hydrophobic pi-pi interactions at Phe699 with 4.33Å, 4,47Å and 5.64Å, and a pi-alkyl interaction with Arg817 (4.26Å) were also observed. The interaction of PZA and EGFR is shown in Fig. 3G–I.

**Table 3** Binding affinity (kcal/mol) of quinolone- and acridine-based drugs and designed derivatives with protein targets of breast cancer

| S. No | Drugs and their designed derivatives | Binding affinity (kcal/mol) | | | |
|---|---|---|---|---|---|
| | | EGFR | HER2 | Topoisomerase IIα | Topoisomerase IIβ |
| 1 | NRT | –7.7 | –7.8 | –6.9 | –6.4 |
| 2 | AMS | –6.9 | –6.8 | –7.9 | –7.2 |
| 3 | PZA | –6.4 | –6.6 | –7.1 | –7.0 |
| 4 | NRT1 | –8.3 | –8.0 | –7.9 | –7.8 |
| 5 | AMS1 | –9.5 | –9.4 | –10.1 | –9.9 |
| 6 | PZA1 | –7.1 | –7.9 | –7.9 | –7.7 |

NRT, AMS and PZA showed the binding score of -7.8 kcal/mol, -6.8 kcal/mol and -6.6 kcal/mol, respectively, against HER2. From here, it is obvious that NRT had the highest affinity among the three ligands binding to HER2. NRT formed a conventional hydrogen bond with Cys805 with 2.16Å, carbon-hydrogen bond with Arg849 (3.78Å), alkyl interactions with Cys805 and Arg849 (4.49Å and 4.53Å, respectively), pi-alkyl interactions with Val734 (4.58Å), Cys805 (4.74Å), Ala751 (4.79Å), Arg849 (4.97Å), Phe731 (5.14Å) and Leu852 (5.32Å). The interaction of NRT and HER2 is shown in Fig. 4A–C. The interactions of AMS and HER2 are shown in Fig. 4D–F. AMS formed conventional hydrogen bonds with Lys753 (2.57Å, 2.78Å) and Arg849 (2.72Å). It also formed pi-anion and pi-sigma interaction with Asp863 with 3.35Å and 3.93Å, respectively. AMS had alkyl interaction with HER2 at Val734 (4.91Å) and pi-alkyl hydro-phobic interaction with Lys753 (3.99Å, 4.08Å, and 5.15Å), Leu796 (5.23Å), Val734 (4.89Å) and Ala751 (5.22Å). PZA formed strong hydrogen bonds with HER2 at Cys805 and Asp863, with distances of 2.42Å and 2.61Å, respectively. PZA also formed carbon-hydrogen bonds with Leu796 (3.66Å) and Gly732 (3.76Å). Besides, it formed pi-sigma interactions with Val734 at 3.80Å, and alkyl interaction with Lys753 (4.24Å) and Leu796 (4.71Å). PZA also formed pi-alkyl interactions with Val 734 (4.44Å and 5.13Å), Ala751

**Table 4** Amino acids of protein targets of breast cancer involved in interactions with quinolone- and acridine-based drugs and designed derivatives

| Enzymes | NRT | AMS | PZA | NRT1 | AMS1 | PZA1 |
|---|---|---|---|---|---|---|
| | **Amino acids involved in the interaction** | | | | | |
| **EGFR** | | | | | | |
| Hydrogen bond/ C-H bond | Val693, Leu694 | Lys721, Asn818 | Asp831, Asn818 | Phe699, Glu738, Cys773, Asp776, Asp813, Lys851 | Ala698, Asn818 | Lys721 |
| Hydrophobic | Phe699, Cys773, Arg817 | Cys773, Arg817 | Phe699, Arg817 | Phe699, Cys773, Lys851 | Phe699, Ile735, Cys773, Arg817 | Phe699, Cys773 |
| Others | | Asp831 | Cys773, Asp831 | Asp831 | Lys721, Glu738, Asp831 | Arg817, Arg831 |
| **HER2** | | | | | | |
| Hydrogen bond/ C-H bond | Cys805, Arg849 | Lys753, Arg849 | Gly732, Leu796, Cys805, Asp863 | Leu796, Arg849, Thr862 | Ala730 | Cys805 |
| Hydrophobic | Phe731, Val734, Ala751, Cys805, Arg849, Leu852 | Val734, Ala751, Lys753, Leu796, Asp863 | Val734, Ala751, Lys753, Leu796, Cys805 | Cys805, Arg849, Val884, Pro885 | Ala730, Phe731, Val734, Ala751, Lys753, Leu852, Val884, Pro885 | Phe731, Val734, Ala751, Cys805, Phe1004 |
| Others | | Asp863 | | Asp863 | Asp863 | |
| **Topoisomerase IIα** | | | | | | |
| Hydrogen bond/ C-H bond | Asp683, Ser709, Glu712, Asp832 | Lys614, Glu682 | Gln544, Asp545, Lys614, Arg713 | Arg672, Glu682, Ser709, Asp832 | Gln544, Leu685, Lys701, Glu712 | Gln544, Lys614, Ser709, Arg713 |
| Hydrophobic | Pro593, Leu685, Leu705 | Leu592, Pro593 | Phe706, Arg713, His758, His759 | Leu592, Leu705 | Pro593, Leu685, Leu705 | His758, His759 |
| Others | | Arg672 | | | Arg675, Glu682 | |
| **Topoisomerase IIβ** | | | | | | |
| Hydrogen bond/ C-H bond | Gly776 | Lys505, Arg729 | Asp561, Asp726, Ser730, Gly741, Gln742 | Ser480, Glu477, Asp557, Ala768, His775, Gly776 | Arg729 | Ser730, Gly741, Gln742, Ile872 |
| Hydrophobic | Arg729, Lys739, Tyr773, Ala779 | Arg729, Lys739, Pro740, His775, Ala779 | Arg729 | Ala768 | Arg729, Lys739, Pro740, Ala779, Leu845 | His775, Ala779, Ile872 |
| Others | Arg561, Arg729 | Arg729 | | | Glu853, Lys744 | Arg729 |

(4.91Å) and Cys805 (5.08Å). Figure 4G–I shows the interactions between PZA and HER2.

For the binding to topoisomerase IIα, the greatest binding affinity was observed in AMS (binding score: –7.9 kcal/mol), followed by PZA (binding score: –7.1 kcal/mol) and lastly NRT (binding score: –6.9 kcal/mol). Figure 5A–C shows the interactions between NRT and topoisomerase IIα. NRT formed strong hydrogen bonding with Glu712 (2.50Å) and Asp683 (2.43Å) and weak carbon-hydrogen bonding with Ser709 (2.94Å) and Asp832 (3.44Å). NRT also formed alkyl interaction with amino acid Leu685 (3.88Å) and Leu705 (4.78Å), and pi-alkyl interactions with Pro593 (4.69Å) and Leu705 (4.61Å) of topoisomerase IIα protein. AMS formed predominant hydrogen bonding with Lys614 and Glu682 with the distances of 2.96Å and 2.11Å, respectively. It also interacted with the amino acid of Arg672 by pi-cation interaction (3.94Å), with Leu592 (5.16Å), Pro593 (4.86Å, 5.14Å) by pi-alkyl interaction. Figure 5D–F shows the interactions between AMS and topoisomerase IIα. Compared to AMS and NRT, PZA had shown different types of interaction with topoisomerase IIα. PZA. formed a strong hydrogen bond with Gln544 (2.24Å), weak carbon-hydrogen bonds with Arg713 (3.58Å), Lsy614 (3.35Å, 3.78Å) and Asp545 (3.62Å), and a pi-hydrogen bond with Gln544 (4.04Å). Figure 5G–I shows the interactions between PZA and topoisomerase

**Table 5** Donor–acceptor pairs in hydrogen bond formation

| Enzyme | Compounds | Type | H-Donor | H-Acceptor |
|---|---|---|---|---|
| **EGFR** | NRT | H-bond | UNK1:NH | Leu694:O |
| | | C-H bond | UNK1:C | Val693:O |
| | AMS | H-bond | Lys721:N | UNK1:O |
| | | | UNK1:C | Asn818:O |
| | PZA | C-H bond | UNK1:C | Asn818:O |
| | | | UNK1:C | Asp831:OD2 |
| | NRT1 | H-bond | UNK1:NH | Asp813:O |
| | | | UNK1:NH | Lys851:O |
| | | | UNK1:OH | Cys773:O |
| | | | UNK1:OH | Asp776:O |
| | | C-H bond | UNK1:C | Phe699:O |
| | | | UNK1:C | Glu738:O |
| | AMS1 | H-bond | UNK1:NH | Ala698:O |
| | | | UNK1:NH | Asn818:O |
| | PZA1 | H-bond | Lys721 | UNK1:O |
| **HER2** | NRT | H-bond | Cys805:N | UNK1:N |
| | | C-H bond | Arg849:NE | UNK1:O |
| | AMS | H-bond | Lys753:N | UNK1:O |
| | | | ARG849:NE | UNK1:O |
| | PZA | H-bond | Cys805:N | UNK1:O |
| | | | UNK1:NH | Asp863:OD2 |
| | | C-H bond | UNK1:C | Leu796:O |
| | | | UNK1:C | Gly732:O |
| | NRT1 | H-bond | UNK1:NH | Arg849:O |
| | | C-H bond | UNK1:C | Leu796:O |
| | | | UNK1:C | Thr862:O |
| | AMS1 | pi-donor hydrogen bond | UNK1 | Ala730:O |
| | PZA1 | H-bond | Cys805:N | UNK1:O |
| **Topoisomerase IIα** | NRT | H-bond | UNK1:NH | Glu712:O |
| | | | UNK1:NH | Asp683:O |
| | | C-H bond | UNK1:C | Ser709:O |
| | | | UNK1:C | Asp832:O |
| | AMS | H-bond | Lys614:N | UNK1:O |
| | | | UNK1:NH | Glu682:O |
| | PZA | H-bond | UNK1:NH | Gln544:O |
| | | C-H bond | Arg713:C | UNK1:O |
| | | | UNK1:C | Lsy614:O |
| | | | UNK1:C | Asp545:O |
| | | pi-donor hydrogen bond | UNK1 | Gln544:O |
| | NRT1 | H-bond | Ser709:N | UNK1:O |
| | | | Arg672:N | UNK1:O |
| | | | UNK1:OH | Glu682:O |

**Table 5** (continued)

| Enzyme | Compounds | Type | H-Donor | H-Acceptor |
|---|---|---|---|---|
| | | C-H bond | UNK1:C | Glu682:O |
| | | pi-donor hydrogen bond | UNK1 | Asp832:O |
| | AMS1 | H-bond | UNK1:NH | Lys701 |
| | | | UNK1:NH | Glu712 |
| | | pi-donor hydrogen bond | UNK1 | Gln544:O |
| | | | UNK1 | Leu685:O |
| | PZA1 | | UNK1:NH | Gln544:O |
| | | | Lys614:N | UNK1:O |
| | | | Arg713:N | UNK1:O |
| | | C-H bond | Ser709:NE | UNK1:O |
| **Topoisomerase IIβ** | NRT | H-bond | Gly776:N | UNK1:O |
| | AMS | H-bond | Lys505:N | UNK1:O |
| | | | UNK1:NH | Arg729:O |
| | PZA | H-bond | Gln742:N | UNK1:O |
| | | | Gly741:N | UNK1:O |
| | | C-H bond | UNK1:C | Asp726:O |
| | | pi-donor hydrogen bond | UNK1 | Ser730:O |
| | NRT1 | H-bond | UNK1:NH | Glu477:O |
| | | | His775:N | UNK1:N |
| | | | Gly776:N | UNK1:N |
| | | | UNK1:OH | Ala768:O |
| | | C-H bond | UNK1:C | Asp557:O |
| | | | UNK1:C | Glu477:O |
| | | | Ser480:N | UNK1:O |
| | AMS1 | H-bond | UNK1:NH | Arg729:O |
| | PZA1 | H-bond | Gly741:N | UNK1:O |
| | | | Gln742 :N | UNK1:O |
| | | | Ile872:N | UNK1:O |
| | | pi-donor hydrogen bond | UNK1 | Ser730:O |

IIα. PZA formed hydrophobic interaction with topoisomerase IIα by forming pi–pi stack with His758 (5.18Å), and pi–pi T-shaped with His 759 (4.77Å, 4.98Å). Other than that, it also formed pi-alkyl with Phe706 (4.96Å) and Arg713 (5.27Å) of topoisomerase IIα.

Among the three drugs, AMS showed the highest binding affinity towards topoisomerase IIβ with a –7.2 kcal/mol binding score, followed by PZA with a slightly lower binding affinity with a –7.0 kcal/mol, and lastly, NRT with a binding score of –6.4 kcal/mol. NRT showed a prominent hydrogen bond interaction to topoisomerase IIβ at Gly776 (1.91Å), pi-cation at Arg729 (4.89Å), pi-anion at Asp561 (3.72Å) and pi–pi T-shaped interaction at Tyr773 (5.75Å). Moreover, an alkyl interaction was observed at Lys739 (4.48Å), and pi-alkyl interaction was observed at Arg729 and Ala779 with the distance of 5.11Å and 4.59Å, respectively. Figure 6A–C shows the interactions between NRT and topoisomerase IIβ. AMS formed a permanent hydrogen bond interaction at Lys505 (2.85Å). At Arg729, there were three different interactions formed by AMS, which were permanent hydrogen

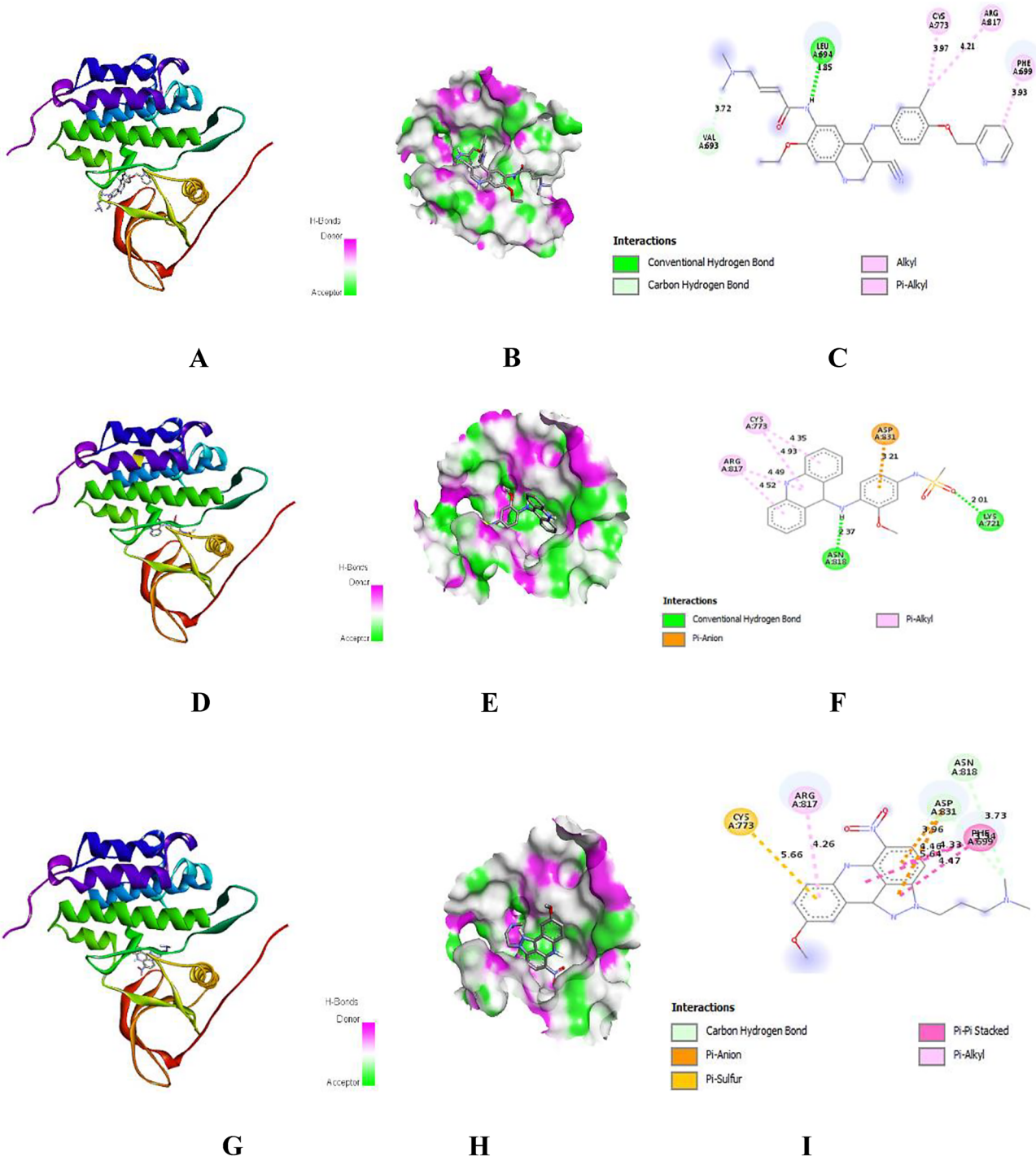


**Fig. 3** **A**, **D**, **G**) 3D interaction; **B**, **E**, **H**) docking pose of hydrogen bonding interaction; **C**, **F**, **I**) 2D interaction diagram of NRT, AMS and PZA with EGFR

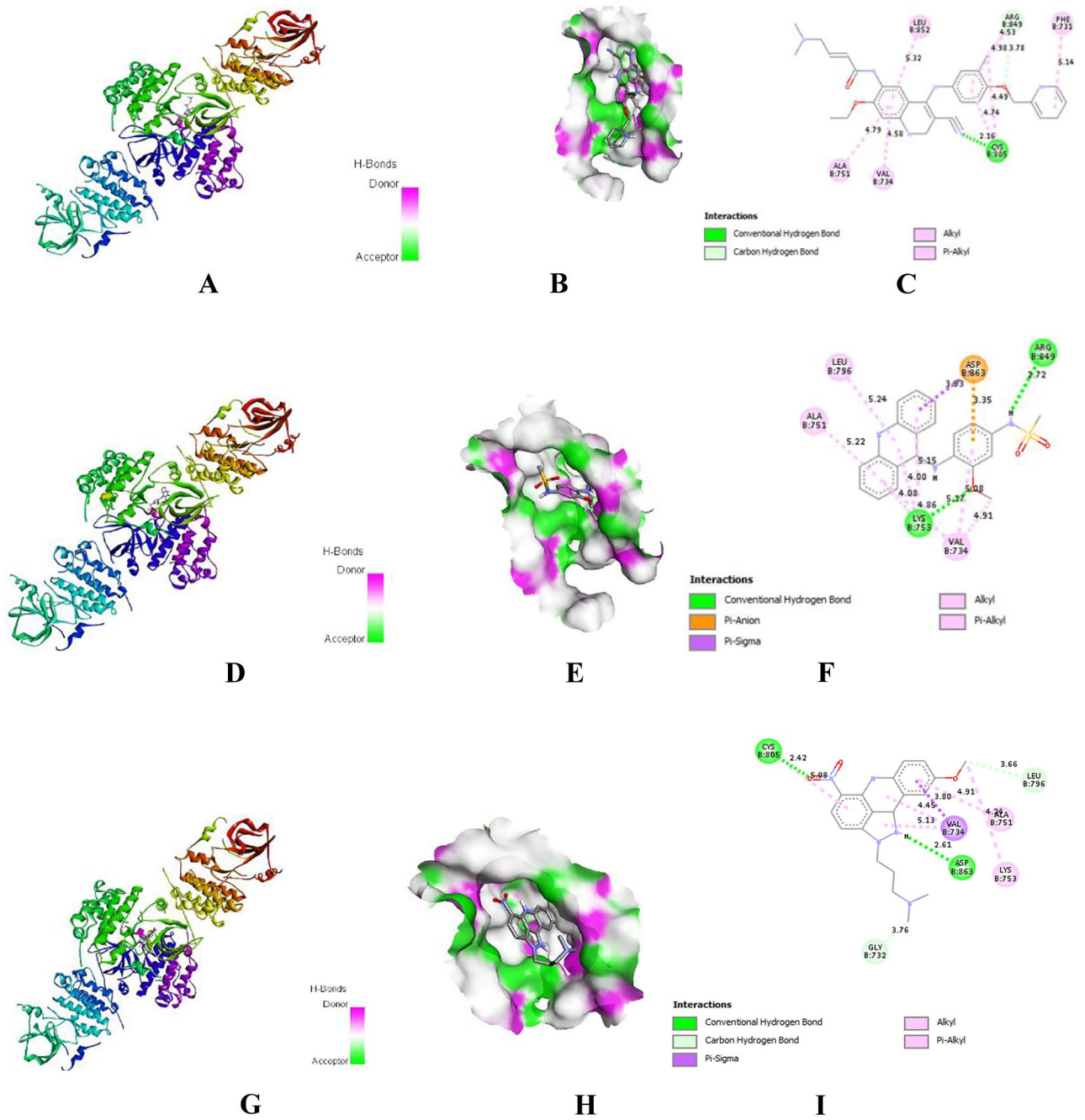


**Fig. 4** **A**, **D**, **G**) 3D interaction; **B**, **E**, **H**) docking pose of hydrogen bonding interaction; **C**, **F**, **I**) 2D interaction diagram of NRT, AMS and PZA with HER2

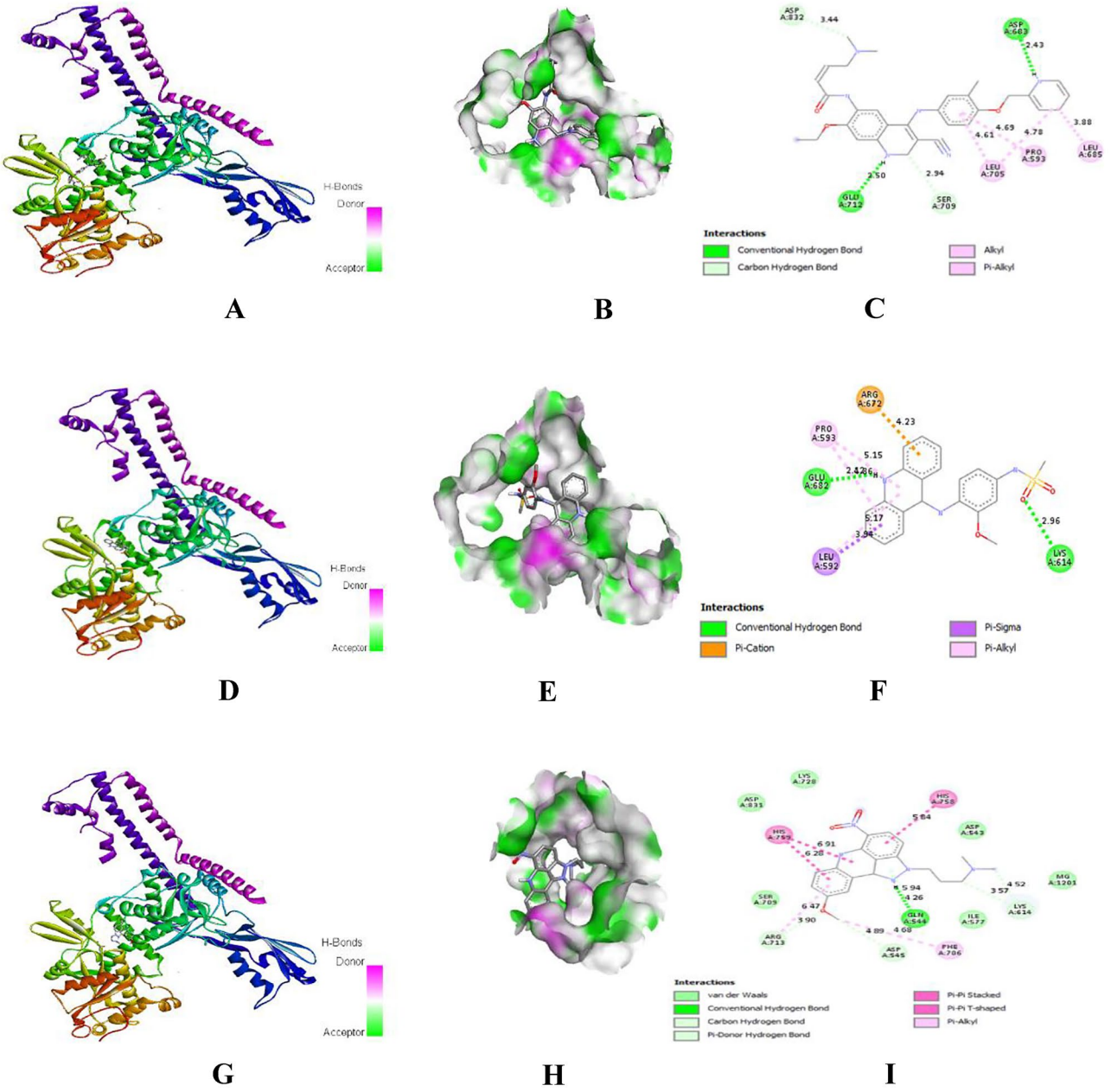


**Fig. 5** **A**, **D**, **G**) 3D interaction; **B**, **E**, **H**) docking pose of hydrogen bonding interaction; **C**, **F**, **I**) 2D interaction diagram of NRT, AMS and PZA with topoisomerase IIα

bonding, pi-cation and pi-sigma interaction at 2.85Å, 4.49Å and 3.56Å, respectively. Pi–pi T-shaped interaction was also observed at His775 (4.95Å), and pi-alkyl interactions were observed at Arg729(4.83Å), Ala779 (4.58Å), Pro740 (5.30Å) and Lys739 (5.49Å). The interactions between A.M.S. and topoisomerase IIβ are shown in Fig. 6D–F. PZA formed permanent hydrogen bonding at Gly741 (2.58Å) and Gln742 (1.94Å), weak carbon-hydrogen bonding at Asp561 (3.48Å) and Asp726 (3.68Å), and a pi-donor hydrogen interaction at Ser730 (2.43Å). Pi-alkyl were also observed at Arg729 (4.32Å, 4.71Å and 4.83Å). Figure 6G–I shows the interactions between PZA and topoisomerase IIβ.

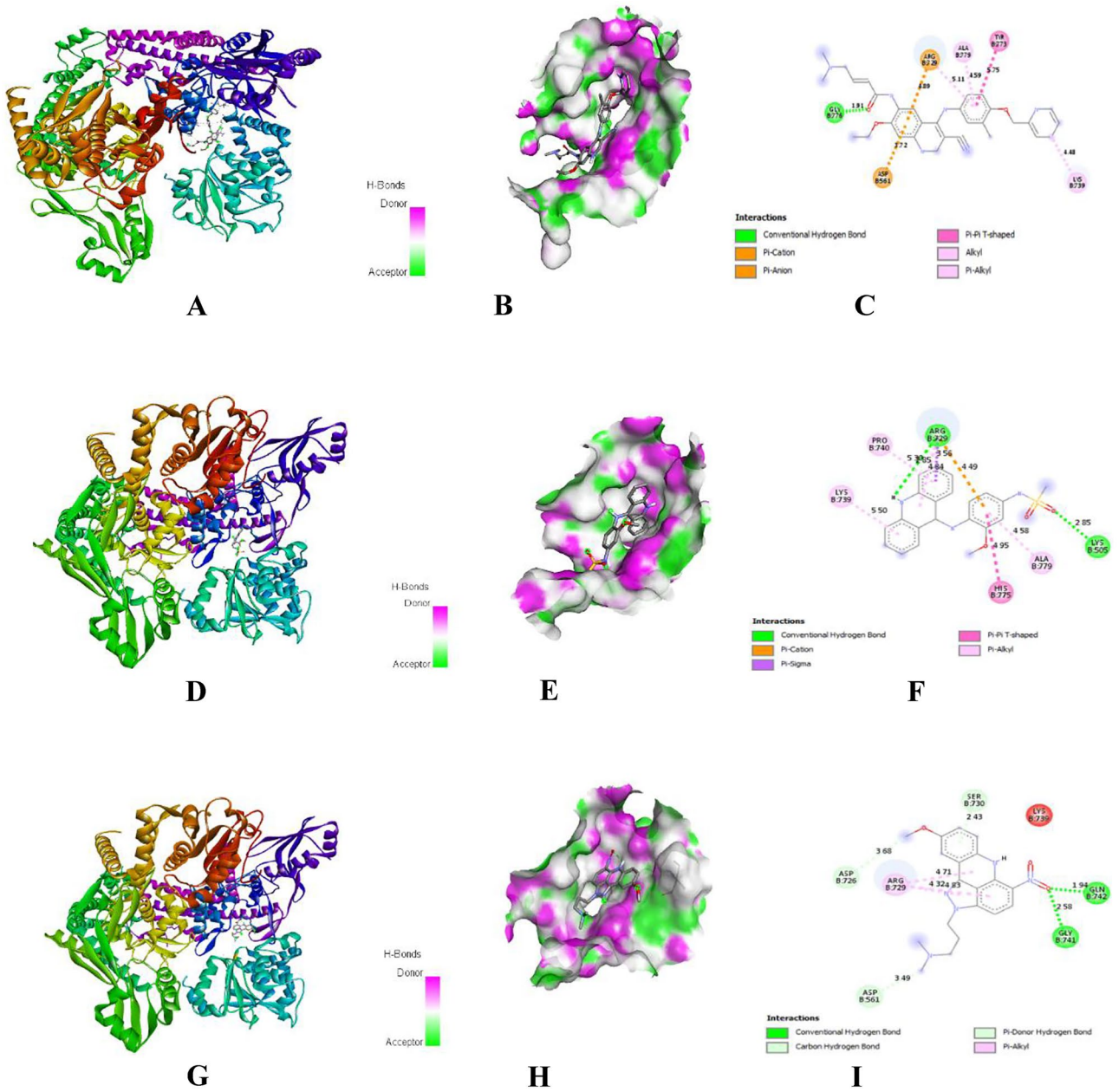


**Fig. 6** **A**, **D**, **G**) 3D interaction; **B**, **E**, **H**) docking pose of hydrogen bonding interaction; **C**, **F**, **I**) 2D interaction diagram of NRT, AMS and PZA with topoisomerase IIβ

## Docking results of designed quinoline and acridine derivatives

The binding scores are shown in Table 3, and the amino acids that interacted with chemically designed quinoline derivatives are shown in Table 4.

AMS1 had shown the required lowest binding energy for binding to the EGFR target, with the binding score –9.5 kcal/mol, followed by NRT1 with the binding score of –8.3 kal/mol and lastly, PZA1 with the binding score of –7.1 kcal/mol. Figure 7A–C shows the interactions between NRT1 and 1M17. NRT1 formed strong hydrogen bonds with Asp776 (2.49Å), Lys851 (2.63Å), Asp813 (2.83Å) and Cys773 (2.96Å), weak car-bon-hydrogen bond with Glu738 (3.38Å) and Phe699 (3.51Å), pi-anion interactions with Asp831 (3.78Å and 3.95Å), pi-sigma interaction and pi–pi stacked interaction with Phe699 (3.44Å, 5.43Å, respectively), alkyl interaction with Cys773 (5.11Å) and pi-alkyl interaction

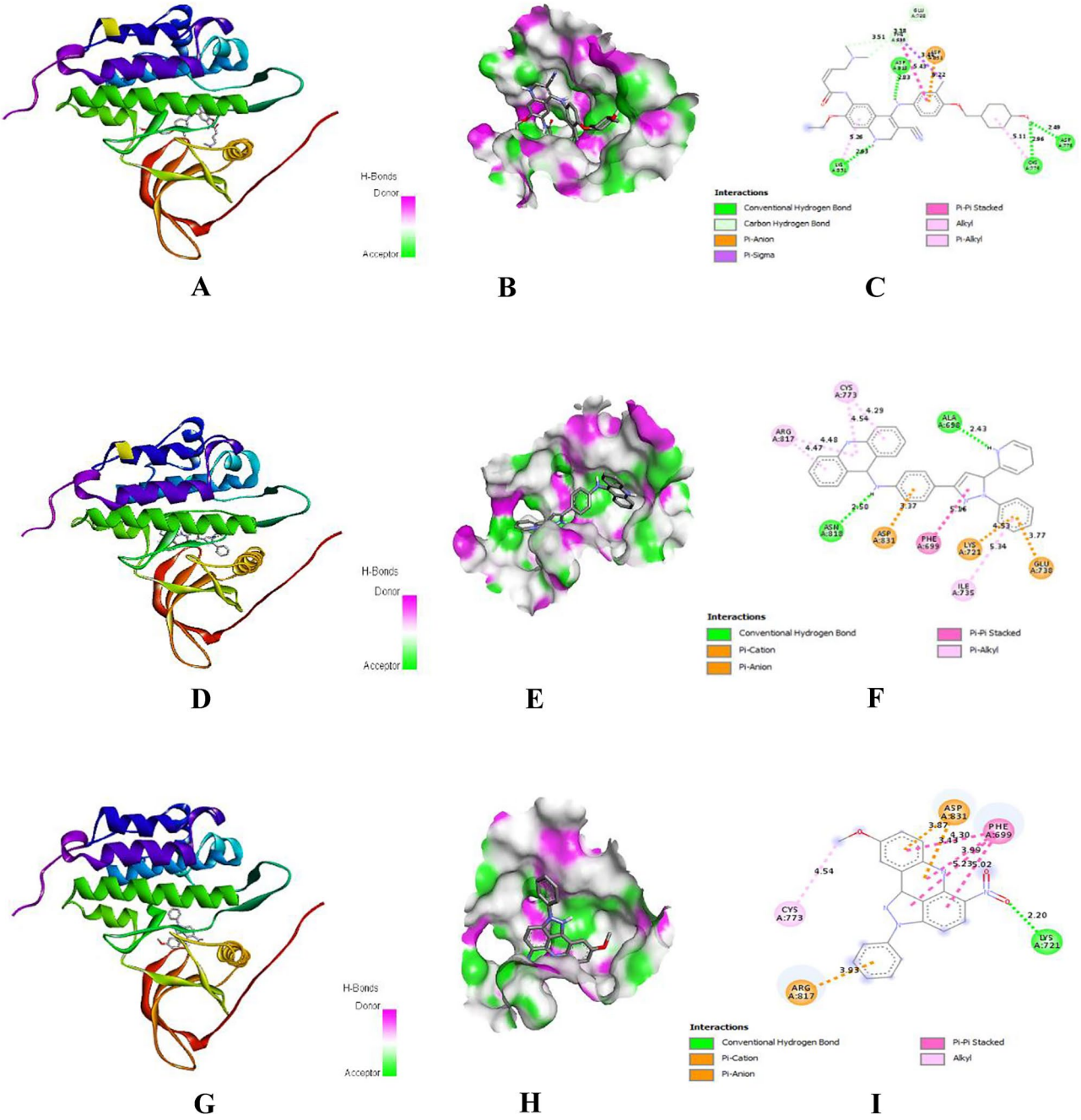


**Fig. 7** **A**, **D**, **G**) 3D interaction; **B**, **E**, **H**) docking pose of hydrogen bonding interaction; **C**, **F**, **I**) 2D interaction diagram of NRT1, AMS1 and PZA1 with EGFR

with Lys851 (5.26Å). AMS1 formed strong hydrogen bonds with Ala698 (2.43Å) and Asn818 (2.49Å), pi-cation interaction with Lys721 (4.57Å), pi-anion interactions with Asp831 (3.36Å) and Glu738 (3.76Å), pi–pi stacked interaction with Phe699 (5.15Å) and pi-alkyl interaction with Cys773 (4.29Å and 4.54Å), Arg817 (4.47Å and 4.48Å) and Ile735 (5.34Å). Figure 7D–F shows the interactions between N.R.T. and EGFR. PZA1 formed a conventional hydrogen bond with Lys721 (2.19Å), pi-cation interaction with Arg817 (3.93Å), pi-anion with Asp831 (3.42Å and 3.86Å), pi–pi stacked interaction with Phe699 (3.99Å, 4.30Å, 5.02Å and 5.23Å) and alkyl interaction with Cys773 (4.54Å). The interaction between PZA1 and EGFR is shown in Fig. 7G–I.

The three designed drugs NRT1, AMS1 and PZA1 showed a binding score of -8.0 kcal/mol, -9.4 kcal/mol and -7.9 kcal/mol, respectively, binding towards HER2.

Figure 8A–C shows the interactions between NRT1 and HER2. NRT1 formed a conventional hydrogen bond with Arg849 (2.17Å), carbon-hydrogen bond with Thr862 (3.35Å) and Leu796 (3.51Å), pi-anion interaction with Asp863 (4.53Å), alkyl interactions with Pro885 (5.25Å) and Val884 (5.43Å) and pi-alkyl interactions with Cys805 (4.51Å) and Arg849 (4.96Å). Figure 8D–F shows the interactions between AMS1 and HER2. AMS1 formed a pi-donor hydrogen bond interaction with Ala730 (2.81Å), pi-anion interactions with Asp863 (3.36Å, 4.47Å), and a pi-sigma interaction with Val734 (3.67Å). AMS1 also had pi–pi T-shaped interaction with Phe731 (4.86Å and 5.13), alkyl interactions with Ala751 (4.36Å) and Leu852 (4.63Å) and pi-alkyl hydrophobic interactions with Ala730 (4.12Å and 5.30Å), Lys753 (4.21Å), Val884 (4.93Å and 5.03Å) and Pro885 (5.04Å). Figure 8G–I shows the interactions between PZA1 and HER2. PZA1 formed conventional hydrogen bonds with Cys805 (1.83Å and 2.86Å), pi-sigma interactions with Cys805 (3.85Å) and Val734 (4.00Å), and pi–pi stacked interaction with Phe1004 (5.51Å). Other than

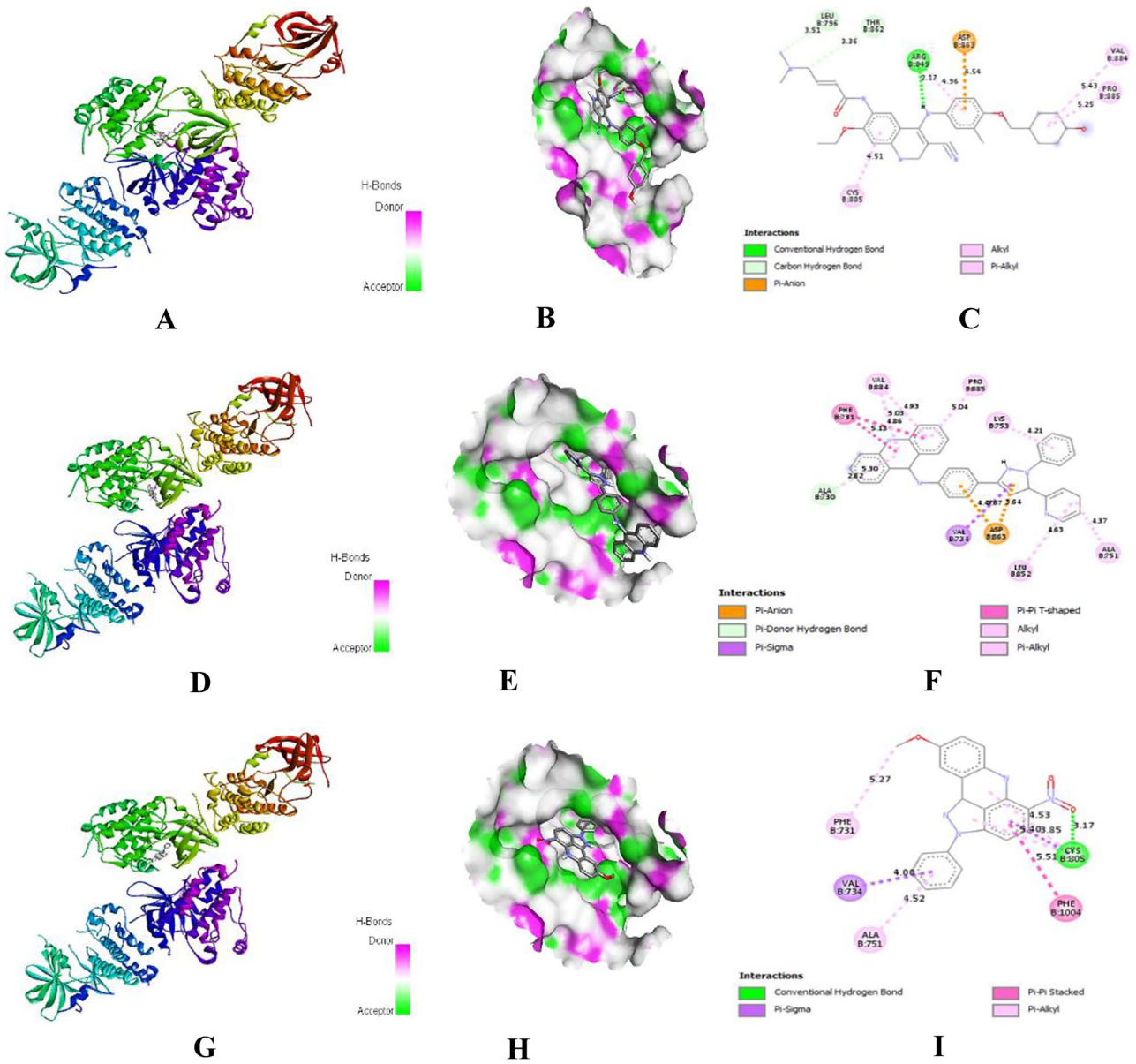


**Fig. 8** **A**, **D**, **G**) 3D interaction; **B**, **E**, **H**) docking pose of hydrogen bonding interaction; **C**, **F**, **I**) 2D interaction diagram of NRT1, AMS1 and PZA1 with HER2

that, PZA1 also formed pi-alkyl interactions with Ala751 (4.51Å), Cys805 (4.53Å and 5.39Å) and Phe731 (5.27Å).

In the binding interaction with topoisomerase IIα, AMS1 showed the highest binding affinity, with a –10.1 kcal/mol binding score. The binding score for both NRT1 and PZA1 was the same, which was –7.9 kcal/mol. Figure 9A–C shows the interactions be-tween NRT1 and topoisomerase IIα. NRT1 formed strong hydrogen bonds with Glu682 (1.94Å), Ser709 (3.02Å) and Arg672 (3.26Å). It also formed a weak carbon-hydrogen bond with Glu682 (3.76Å). Other than that, it formed a pi-donor hydrogen bond with Asp832 (3.99Å), a pi-sigma interaction with Leu592 (3.86Å) and an alkyl interaction with Leu705 (4.34Å). AMS1 formed strong hydrogen bonds

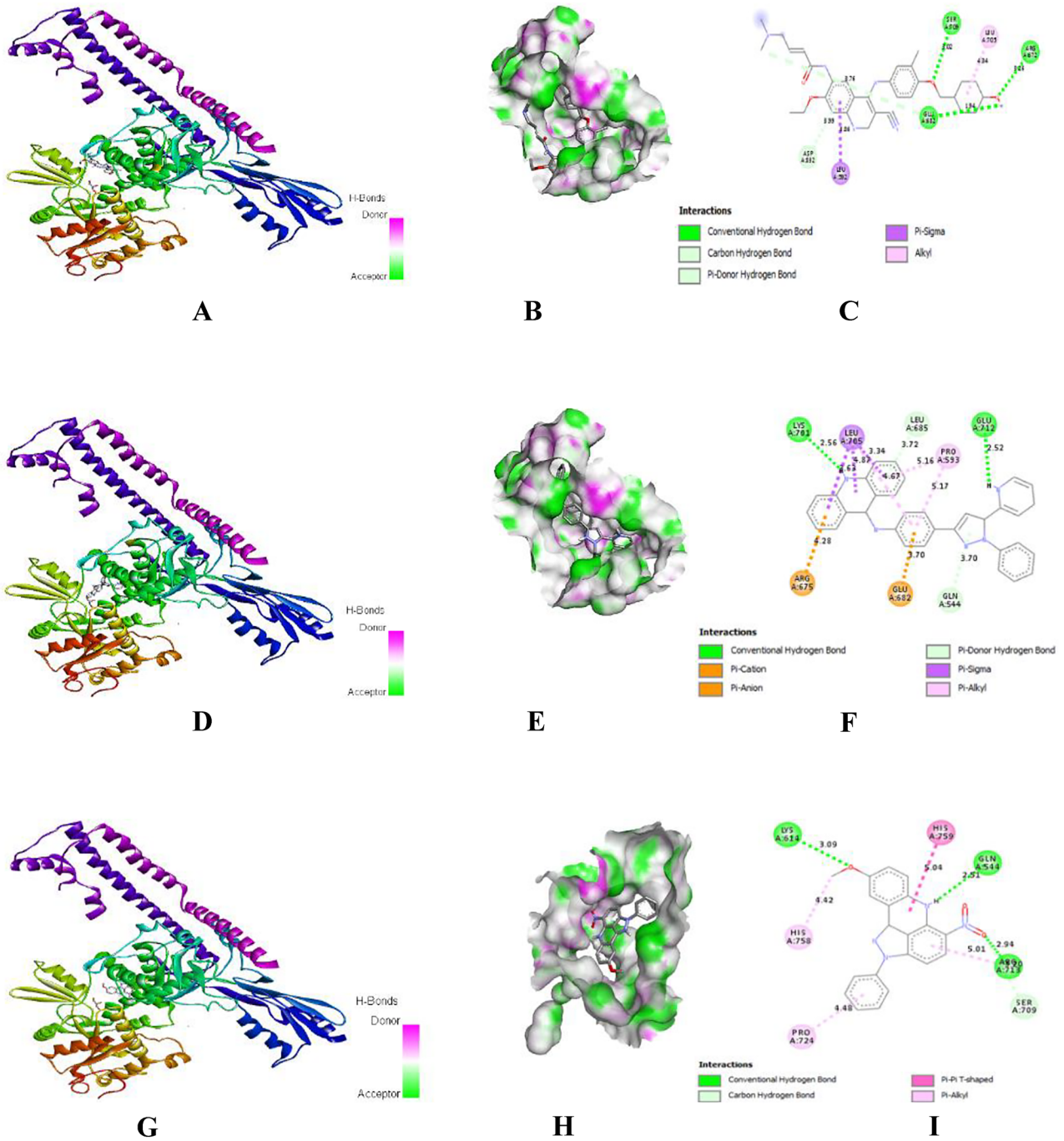


**Fig. 9** **A**, **D**, **G**) 3D interaction; **B**, **E**, **H**) docking pose of hydrogen bonding interaction; **C**, **F**, **I**) 2D interaction diagram of NRT1, AMS1 and PZA1 with topoisomerase IIα

with Glu712 (2.52Å) and Lys701 (2.56Å). AMSA1 also formed a pi-cation interaction with Arg675 (4.28Å) and a pi-anion interaction with Glu682 (3.70Å). However, it formed pi-donor hydrogen bonds with Gln544 and Leu685 (3.70Å and 3.72 Å, respectively), pi-sigma interactions with Leu705 (3.34Å, 3.40Å, 3.59Å and 3.63Å), and pi-alkyl interactions with Leu705 (4.67Å), Leu685 (5.12Å) and Pro593 (5.16Å and 5.17Å). Figure 9D–F shows the interactions between AMS1 and topoisomerase IIα. PZA1 formed strong hydrogen bonds with Gln544 (2.51Å), Arg713 (2.94Å) and Lys614 (3.09Å), and weak carbon-hydrogen bonds with Ser709 (3.20Å) and Arg713 (3.48Å). It also formed pi–pi T-shaped interactions with His759 (5.04Å) and a pi-alkyl inter-action with His758 (4.42Å). Figure 9–I shows the interactions between PZA1 and topoisomerase IIα.

The binding affinity to topoisomerase IIβ was found to be highest for AMS1 (binding score: –9.9 kcal/mol), and NRT1 and PZA1 showed roughly the same binding score, which was –7.8 kcal/mol and –7.7 kcal/mol, respectively. NRT1 formed conventional hydrogen bonds with Ala768 (2.00Å), Glu477 (2.12Å), His775 (2.18Å) and Gly776 (2.79Å) and car-bon-hydrogen bonds with Glu477 (3.53Å), Ser480 (3.57Å) and Asp557 (3.78Å). It also formed alkyl interaction with Ala768 (4.89Å). Figure 10A–C shows the interactions between NRT1 and topoisomerase IIβ. AMS1 showed a conventional hydrogen bonding with Arg729 (3.06Å). It also formed pi-cation interaction with Lys744 (2.68Å) and pi-anion interactions with Glu853 (4.29Å and 4.30Å). Other than that, AMS1 also formed a pi-sigma interaction with Arg729 (3.71Å), an alkyl interaction with Lys739 (4.40Å), and pi-alkyl interactions with Ala779 (4.06Å), Pro740 (4.46Å), Arg729 (4.81Å), Pro740 (4.93Å) and Leu845 (5.28Å). Figure 10D–F shows the interactions between AMS1 and topoisomerase IIβ. Figure 10G–I shows the interactions between PZA1 and topoisomerase IIβ. PZA1 formed strong hydrogen bonds with Gly741, Gln742 and Ile872 (2.38Å, 2.47Å and 2.78Å, respectively), a pi-cation interaction with Arg729 (4.37Å), a pi-donor hydrogen bond with Ser730 (2.68Å), a pi–pi T-shaped interaction with His775 (4.99Å), an alkyl interaction with Ile872 (4.10Å) and pi-alkyl interactions with Ala779 (4.75Å).

NRT is a pan-Her inhibitor, which irreversibly binds to tyrosine kinase of HER family protein and forms a covalent complex, which suppresses the tyrosine kinase activity of EGFR and HER2. NRT competes with high concentrations of cellular ATP [32]. This results in a decrease in phosphorylation activation of the downstream signalling pathway, which eventually inhibits tumour cell proliferation and decreases the survival of the cells [33]. A higher dose of NRT could lead to cell apoptosis [32]. NRT is an oral tyrosine kinase inhibitor. NRT interacted with Cys773 in EGFR and Cys805 in HER2 at the cleft of the ATP binding site of the kinase domain of HER family, causing NRT to be highly specific in selective binding both EGFR and HER2 [33]. This can be observed in this molecular docking study as NRT showed higher binding efficacy in EGER and HER2, with binding score –7.7 kcal/mol and –7.8 kcal/mol, respectively, while lower binding affinity in topoisomerase IIα and topoisomerase IIβ, with binding score -6.9 kcal/mol and -6.4 kcal/mol, respectively.

In the designed molecule NRT1, NRT was designed to bind to tyrosine kinase with a higher affinity to prevent receptor phosphorylation and give a stronger cell proliferation inhibition effect. Both the interaction of NRT on Cys773of EGFR and Cys805 of HER2 was retained. In EGER, NRT reacts with Cys773 by alkyl interaction with 3.97Å. After modification to NRT1 molecules, NRT1 reacted with Cys773 with alkyl interaction (5.11Å) and strong hydrogen bonding (2.94Å) at the hydroxyl group added after drug designation, which led to higher specificity of this drug towards EGFR. The hydroxyl group added after the drug was designed also formed a strong hydrogen bond with Asp776 (2.49Å). Overall, NRT1 formed more hydrogen bonding (six hydrogen bonds) than NRT (two hydrogen bonds) and more hydrophobic interaction towards EGFR leading to improvement of binding score form –7.7 kcal/mol (NRT) to –8.3 kcal/mol (NRT1). In HER2, NRT reacts with Cys805 through hydrogen bond (2.16Å), alkyl interaction (4.49Å) and pi-alkyl interaction (4.74Å) with a binding score of –7.8 kcal/mol. Besides at reaction at Cys805, NRT mostly forms hydrophobic interaction with HER2 like pi-alkyl bonds. After modification of the drug, NRT1 formed a slightly higher binding score, –8.0 kcal/mol. The number of hydrogen bonds increased from two to three after structure modification. The appearance of pi-anion interaction with Asp863 and different hydrophobic interactions between NRT1 and HER2 were observed, which led to an increase in binding affinity. However, the reaction of NRT1 on Cys805 was lesser than that of NRT as there is only a pi-alkyl interaction (4.51Å) observed. This shows that NRT1 is not that high selectively binding to HER2 after modification.

In interaction with topoisomerase IIα (PDB ID: 4FM9), NRT formed a hydrogen bond and hydrophobic interaction (alkyl and pi-alkyl), giving a binding score of -6.9 kcal/mol. After drug structure modification, the bonding affinity increased to –7.9 kcal/mol. The improvement of binding affinity may be due to an increase of hydrogen bonding interaction as an additional pi-donor hydrogen bond was observed after drug modification,

whereas in topoisomerase IIβ, the binding score of NRT improved from –6.4 kcal/mol to –7.8 kcal/mol after drug structure modification. NRT interacted with topoisomerase IIβ with hydrogen bonds, electrostatic interactions (pi-cation, pi-anion) and hydrophobic interaction (pi–pi T-shaped, alkyl and pi-alkyl). The binding score

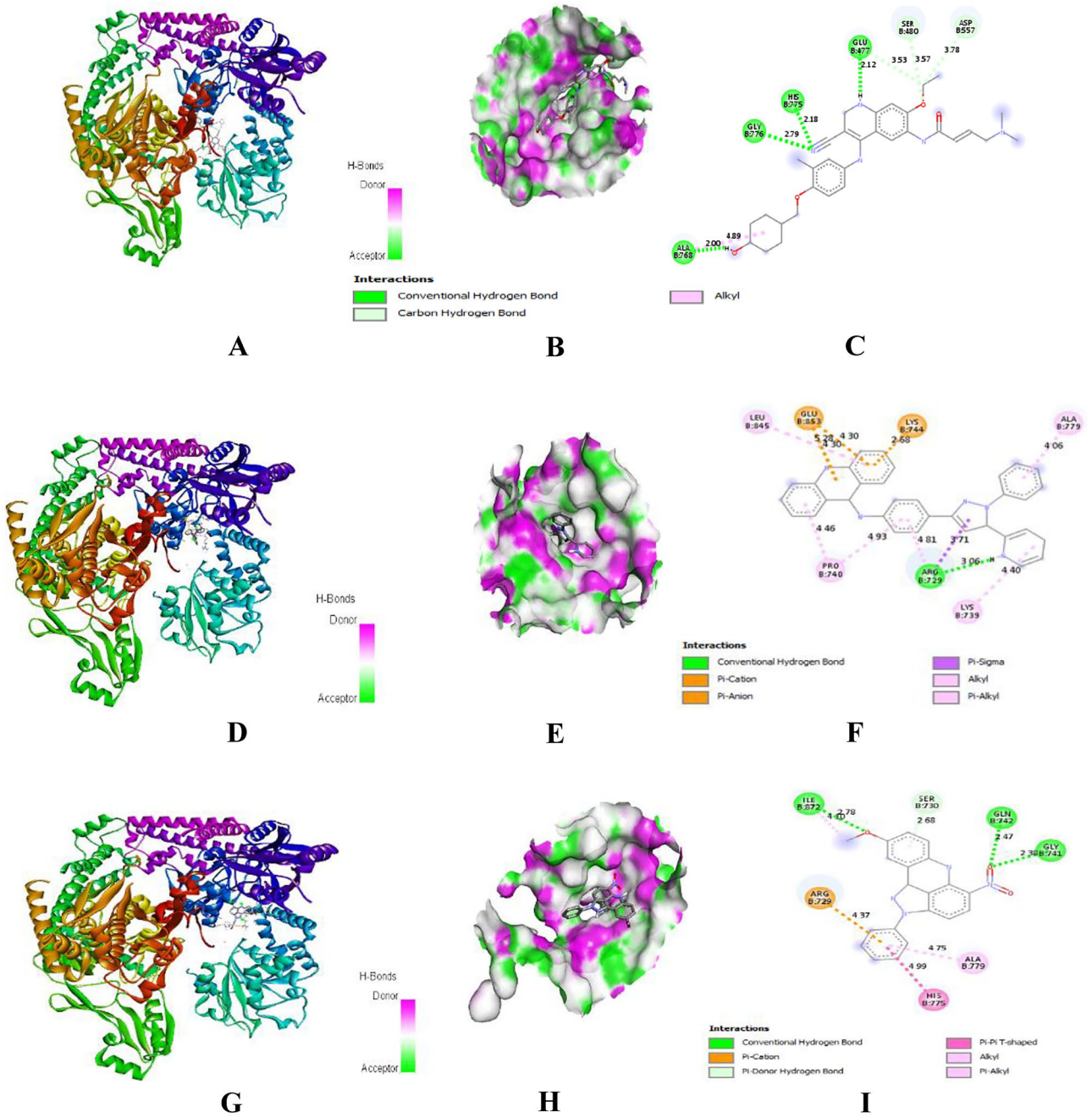


**Fig. 10** **A**, **D**, **G**) 3D interaction; **B**, **E**, **H**) docking pose of hydrogen bonding interaction; **C**, **F**, **I**) 2D interaction diagram of NRT1, AMS1 and PZA1 with topoisomerase IIβ

improved after structure modification as the number of hydrogen bonds interacting between NRT1 and topoisomerase IIβ increased. The number of hydrogen bonds formed by NRT was only one, a conventional hydrogen bond at Gly776 (1.91Å). After structure modification, the number of hydrogen bonds increased to seven which were four conventional hydrogen bonds at His775 (2.18Å), Gly776 (2.79 Å), Glu477 (2.12 Å) and Ala768 (2.00 Å) and carbon-hydrogen bonds at Ser480 (3.57 Å), Glu477 (3.53 Å) and Asp557 (3.78Å).

AMS is demonstrated to function as a topoisomerase II poison. It is used as anti-cancer chemotherapy combined with other drugs [34]. AMS binds to DNA through intercalation; besides interacting with DNA, it also targets and inhibits topoisomerase II. The cytotoxic effect is the highest in the S phase of the cell cycle topoisomerase II level are at the

maximum. AMS is widely used in treating refractory acute Hodgkin's and non-Hodgkin's lymphomas as well as lymphocytic and non-lymphocytic leukaemia. AMS is also used as a treatment option in other type of cancer, including breast cancer. From the chemistry point of view, AMS consists of two moieties; the lower part containing the quinoline group is responsible for DNA intercalation. In contrast, the upper part with the 4'-aminomethanesulfonmanisidide head group is responsible for topoisomerase II inhibitor [34]. The head group involves the poisoning effect via ligand–protein interaction, and it should be effective in forming topoisomerase II-DNA complex without the lower part intercalating body [35]. As the targeted protein in this research focuses on the HER family and topoisomerase II, the drug modification of AMS was done only on the head group without changing the lower part structure. AMS was effective in topoisomerase IIα and topoisomerase IIβ, with a binding score of –7.9 kcal/mol and –7.2 kcal/mol, respectively. Compared to topoisomerase II, the binding to EGFR and HER2 was seemed to be low effective, with the binding score of –6.9 kcal/mol and –6.8 kcal/mol, respectively.

AMS interacted with topoisomerase IIα with various bonding including hydrogen bonds, electrostatic interactions (pi-cation) and hydrophobic interaction (pi-sigma and pi-alkyl), giving a binding score of –7.9 kcal/mol. After drug modification, the binding score increased to –10.1 kcal/mol. Although the number of hydrogen bonds formed of AMS1 with topoisomerase IIα and AMS with topoisomerase IIα is the same, the hydrophobic interaction is more significant in AMS1, and pi-anion interaction, pi-hydrogen bonds that were not obtained in AMS were observed in AMS1. AMS interacted with topoisomerase IIβ with hydrogen bonding, electrostatic interaction (pi-cation), hydrophobic interaction (pi-sigma, pi–pi T-shaped and pi-alkyl) and other interaction such as pi-lone pair interaction. In AMS1, additional pi-anion interactions, pi–pi stacked interactions and alkyl interactions were observed. Thus, the binding score increased from –7.2 kcal/mol to –9.9 kcal/mol.

In EGER (PDB ID: 1M17), AMS showed a binding score of –6.9 kcal/mol; the binding score increased to –9.5 kcal/mol after structure modification. Both AMS and AMS1 showed pi-alkyl binding to Cys773, with distances 4.34Å, 4.93Å and 4.29Å, 4.54Å, respectively. Hydrogen bonding, electrostatic interaction (pi-anion) and hydrophobic interaction (pi-alkyl) were observed in AMS interaction with EGFR, and additional pi-cation interactions and pi–pi stacked interactions were observed in AMS1, whereas in HER2 (PDB ID: 3RCD), AMS showed the least binding affinity, with a –6.8 kcal/mol binding score. The binding score increased to –9.4 kcal/mol after structure modification. Both AMS and AMS1 did not show any binding towards Cys805. AMS interacts with HER2 with hydrogen bonding, electrostatic interaction (pi-anion) and hydrophobic interaction (pi-sigma, alkyl and pi-alkyl). After structure modification, AMS1 showed weaker hydrogen bonding but higher electrostatic interaction (pi-anion), and hydrophobic interaction (pi-sigma, alkyl, and pi-alkyl) and additional pi–pi T-shaped interaction towards HER2. Like AMS, PZA anti-cancer properties are due to its action on DNA intercalation and topoisomerase enzymes. In preclinical data, PZA showed an advantage as it had a cyto-toxic effect on non-cycling cells. Most importantly, it overcame multi-drug resistance in a broad spectrum of human tumour cell lines, including breast cancer tumour cells [36]. However, docking studies on PZA are still minimal as PZA is still under clinical trial for its anti-cancer efficacy and safety. Thus, the binding affinity of PZA on each targeted enzyme was studied, and the drug's structure was modified to increase the binding affinity. PZA formed hydrogen bonds and hydrophobic bonds (pi–pi staked, pi–pi T-shaped and pi-alkyl) when binding to topoisomerase IIα with a binding score of –7.1 kcal/mol. After structure modification, PZA1 produced had a more excellent binding score of –7.9 kcal/mol. Although the hydrophobic interaction decreases after drug structure modification, the modified drug's binding affinity was due to the decreasing bond length and an increasing number of strong hydrogen bonds formed between the drug and topoisomerase IIα. This can be seen as a new strong hydrogen bond formed at Lys614 with the hydroxyl group of the modified drug, which was previously observed as a weak carbon-hydrogen bond in PZA.

In the interaction between PZA and topoisomerase IIβ, only a few types of bonding were observed: hydrogen bonds and hydrophobic bonds (pi-alkyl), giving a binding score of –7.0 kcal/mol. After drug structure modification, a greater binding score was obtained, –7.7 kcal/mol. After drug structure modification, PZA1 showed a variety of interactions on topoisomerase IIβ, including hydrogen bond interactions, hydrophobic interaction (pi-alkyl) and additional pi-donor hydrogen bonding, electrostatic interaction (pi-cation, pi-anion) and hydrophobic interaction (pi-sigma, alkyl, pi–pi T-shaped). The binding of PZA on EGFR involved various bonding including hydrogen bonds, electrostatic interaction (pi-anion) and hydrophobic bonds (pi-sigma, pi–pi stacked and pi-alkyl), giving a binding score of –6.4 kcal/mol. The binding score increased to –7.1 kcal/mol after structural modification. In interaction with HER2, the binding score of PZA was –6.6 kcal/mol and increased to –7.3 kcal/mol after structural modification. Both PZA and PZA1 interacted with HER2 with various bonding, including hydrogen and hydrophobic bonds (pi-sigma and pi-alkyl). Alkyl interaction was observed in P.Z.A. but absent after structure modification, whereas pi–pi stacked interaction was only present after modifications. Looking into the interaction with

Cys805, P.Z.A. formed a hydrogen bond with 2.42Å and pi-alkyl interaction with 5.08Å. After drug modification, PZA1 formed two hydrogen bonds with 1.84Å and 2.87Å and pi-alkyl interaction with 4.53Å and 5.40Å, showing that PZA1 have a higher binding selectivity on HER2 after structural modification.

## Conclusions

In this in silico study, the molecular interaction of neratinib, amsacrine and pyrazoloacridine with various breast cancer enzymes EGFR, HER2, topoisomerase IIα and topoisomerase IIβ was studied. The result obtained found that neratinib had a better binding affinity towards EGFR and HER2 but weaker binding affinity towards topoisomerase IIα and β. On the other hand, amsacrine and pyrazoloacridine were found to have a better binding score in topoisomerase IIα and β instead of EGFR and HER2. Thus, all designed quinolone and acridine derivatives showed improved binding affinity towards various targeted enzymes than the parent drugs. Moreover, all the designed derivatives also show drug-likeness, ADMET and pharmacokinetic properties as like neratinib, amsacrine and pyrazoloacridine. Designed derivative of AMS and PZA showed better predicted $LD_{50}$ than the parent drugs. Hence, these compounds can be further optimized with molecular dynamic studies, will be synthesized and evaluated for in vitro and in vivo anti-breast cancer activity.

**Acknowledgments** The authors acknowledge AIMST University, Malaysia, for providing the necessary facilities to carry out the studies.

**Authors' contributions** Veerasamy Ravichandran and Rohini Karunakaran were involved in the conceptualization; Lai Cong Sing, Anitha Roy, Lok Yong Hui, Chan Sook Mun, Harish Rajak and Veerasamy Ravichandran contributed to the methodology; Lai Cong Sing, Lok Yong Hui and Chan Sook Mun contributed to the writing—original draft preparation; Veerasamy Ravichandran, Rohini Karunakaran, Anitha Roy and Harish Rajak were involved in writing–review and editing; Veerasamy Ravichandran contributed to the supervision. All authors read and approved the final manuscript.

**Funding** This research received no external funding.

**Availability of data and material** All the data and material related to this manuscript were included in the manuscript itself.

## Declarations

**Ethical approval** This work does not contain any studies with human participants or animals.

**Conflict of interests** The authors declare that they have no conflict of interest.

## References

1. GLOBOCAN (2020) New Global Cancer Data. Uicc.org Accessed 10 Sept 2021
2. Siegel RL, Miller KD, Jemal A (2020) Cancer statistics, 2020. CA Cancer J Clin 70:7–30
3. Liu L, Kawashima M, Toi M (2020) Breast cancer in global health: beyond diversity and inequality. International Journal of Surgery: Global Health 3:e32–e32
4. Smith RA, Andrews KS, Brooks D et al (2018) Cancer screening in the United States, 2018: A review of current American Cancer Society guidelines and current issues in cancer screening. CA: Cancer J Clin 68:297–316
5. Bray F, Ferlay J, Soerjomataram I et al (2018) Global cancer statistics 2018: GLOBOCAN estimates of incidence and mortality worldwide for 36 cancers in 185 countries. CA: Cancer J Clin 68:394–424
6. Tao Z, Shi A, Lu C et al (2015) Breast cancer: Epidemiology and etiology. Cell Biochem Biophys 72:333–338
7. Maennling AE, Tur MK, Niebert M et al (2019) Molecular targeting therapy against EGFR family in breast cancer: Progress and future potentials. Cancers (Basel) 11:1826
8. Bhatia P, Sharma V, Alam O et al (2020) Novel quinazoline-based EGFR kinase inhibitors: A review focussing on SAR and molecular docking studies (2015-2019). Eur J Med Chem 204:112640
9. Al-Suwaidan IA, Alanazi AM, Abdel-Aziz AA-M et al (2013) Design, synthesis, and biological evaluation of 2-mercapto-3-phenethylquinazoline bearing anilide fragments as potential antitumor agents: molecular docking study. Bioorg Med Chem Lett 23:3935–3941
10. Damiani RM, Moura DJ, Viau CM et al (2016) Pathways of cardiac toxicity: comparison between chemotherapeutic drugs doxorubicin and mitoxantrone. Arch Toxicol 90:2063–2076
11. Skok Ž, Zidar N, Kikelj D, Ilaš J (2020) Dual inhibitors of human DNA topoisomerase II and other cancer-related targets. J Med Chem 63:884–904
12. Arthur DE (2019) Molecular docking studies of some topoisomerase II inhibitors: Implications in designing of novel anticancer drugs. Radiol Infect Dis 6:68–79
13. Afzal O, Kumar S, Haider MR et al (2015) A review on anticancer potential of bioactive heterocycle quinoline. Eur J Med Chem 97:871–910
14. Abbas SH, Abd El-Hafeez AA, Shoman ME et al (2019) New quinoline/chalcone hybrids as anti-cancer agents: Design, synthesis, and evaluations of cytotoxicity and PI3K inhibitory activity. Bioorg Chem 82:360–377
15. Abu Saleh M, Solayman M, Hoque MM et al (2016) Inhibition of DNA topoisomerase type IIα (TOP2A) by mitoxantrone and its halogenated derivatives: A combined density functional and molecular docking study. Biomed Res Int 2016:6817502
16. El-Sayed MA-A, El-Husseiny WM, Abdel-Aziz NI et al (2018) Synthesis and biological evaluation of 2-styrylquinolines as antitumour agents and EGFR kinase inhibitors: molecular docking study. J Enzyme Inhib Med Chem 33:199–209
17. Gatadi S, Pulivendala G, Gour J et al (2020) Synthesis and evaluation of new 4 (3H)-Quinazolinone derivatives as potential anticancer agents. J Mol Struct 127097
18. Joshi PV, Sayed AA, RaviKumar A et al (2017) 4-Phenyl quinoline derivatives as potential serotonin receptor ligands with antiproliferative activity. Eur J Med Chem 136:246–258
19. Kalirajan R, Sankar S, Jubie S, Gowramma B (2017) Molecular Docking studies and in-silico ADMET Screening of Some novel Oxazine substituted 9-Anilinoacridines as Topoisomerase II Inhibitors. Ind J Pharm Educ 51:110–115

20. Manohar CS, Manikandan A, Sridhar P et al (2018) Drug repurposing of novel quinoline acetohydrazide derivatives as potent COX-2 inhibitors and anti-cancer agents. J Mol Struct 1154:437–444
21. Mirzaei S, Hadizadeh F, Eisvand F et al (2020) Synthesis, structure-activity relationship, and molecular docking studies of novel quinoline-chalcone hybrids as potential anticancer agents and tubulin inhibitors. J Mol Struct 1202:127310
22. Prabhavathi H, Dasegowda KR, Renukananda KH et al (2021) Exploration and evaluation of bioactive phytocompounds against BRCA proteins by in silico approach. J Biomol Struct Dyn 39:5471–5485
23. Ribeiro AG, Almeida SMV de, de Oliveira JF et al (2019) Novel 4-quinoline-thiosemicarbazone derivatives: Synthesis, antiproliferative activity, in vitro and in silico biomacromolecule interaction studies and topoisomerase inhibition. Eur J Med Chem 182:111592
24. Saeed AM, Abdou IM, Salem AA et al (2020) Anti-Cancer Activity and Molecular Docking of Some Pyrano [3, 2 c] quinoline Analogues. Open J Med Chem 10:1–14
25. Sawatdichaikul O, Hannongbua S, Sangma C et al (2012) In silico screening of epidermal growth factor receptor (EGFR) in the tyrosine kinase domain through a medicinal plant compound database. J Mol Model 18:1241–1254
26. Shah SR, Katariya KD, Reddy D (2020) Quinoline-1, 3-Oxazole Hybrids: Syntheses, Anticancer Activity and Molecular Docking Studies. Chemistry Select 5:1097–1102
27. Thirumurugan C, Vadivel P, Lalitha A, Lakshmanan S (2020) Synthesis, characterization of novel quinoline-2-carboxamide based chalcone derivatives and their molecular docking, photochemical studies. Synth Commun 50:831–839
28. Zou M, Li J, Jin B et al (2021) Design, synthesis, and anticancer evaluation of new 4-anilinoquinoline-3-carbonitrile derivatives as dual EGFR/HER2 inhibitors and apoptosis inducers. Bioorg Chem 114:105200
29. Dallakyan S, Olson AJ (2015) Small-molecule library screening by docking with PyRx. Methods Mol Biol 1263:243–250
30. Adeniji SE, Arthur DE, Oluwaseye A (2020) Computational modeling of 4-Phenoxynicotinamide and 4-Phenoxypyrimidine-5-carboxamide derivatives as potent anti-diabetic agent against TGR5 receptor. J King Saud Univ Sci 32:102–115
31. Vianna CP, Azevedo WF (2012) Jr Identification of new potential Mycobacterium tuberculosis shikimate kinase inhibitors through molecular docking simulations. J Mol Model 18:755–764
32. Guo P, Pu T, Chen S et al (2017) Breast cancers with EGFR and HER2 co amplification favor distant metastasis and poor clinical outcome. Oncol Lett 14:6562–6570
33. Feldinger K, Kong A (2015) Profile of neratinib and its potential in the treatment of breast cancer. Breast Cancer (Dove Med Press) 7:147–162
34. Ketron AC, Denny WA, Graves DE, Osheroff N (2012) Amsacrine as a topoisomerase II poison: importance of drug-DNA interactions. Biochemistry 51:1730–1739
35. Sader S, Wu C (2017) Computational analysis of Amsacrine resistance in human topoisomerase II alpha mutants (R487K and E571K) using homology modeling, docking and all-atom molecular dynamics simulation in explicit solvent. J Mol Graph Model 72:209–219
36. Ramaswamy B, Mrozek E, Kuebler JP et al (2011) Phase II trial of pyrazoloacridine (NSC#366140) in patients with metastatic breast cancer. Invest New Drugs 29:347–351



## Authors and Affiliations

**Lai Cong Sing[1] · Anitha Roy[2] · Lok Yong Hui[1] · Chan Sook Mun[1] · Harish Rajak[3] · Rohini Karunakaran[4,5] · Veerasamy Ravichandran[1,5,6]**

Lai Cong Sing
lai.p18091012@student.aimst.edu.my

Anitha Roy
anitharoy2015@gmail.com

Lok Yong Hui
lok.p18090788@student.aimst.edu.my

Chan Sook Mun
chan.p17090806@student.aimst.edu.my

Harish Rajak
harish-dops@yahoo.co.in

Rohini Karunakaran
rohini@aimst.edu.my

[1] Faculty of Pharmacy, AIMST University, Semeling, 08100 Kedah, Malaysia

[2] Center for Transdisciplinary Research, Department of Pharmacology, Saveetha Dental College and Hospitals, Saveetha Institute of Medical and Technical Sciences, Chennai, Tamil Nadu, India

[3] S.L.T. Institute of Pharmaceutical Sciences, Guru Ghasidas University, Bilaspur, India

[4] Faculty of Medicine, AIMST University, Semeling, 08100 Kedah, Malaysia

[5] Centre of Excellence for Biomaterials Science, AIMST University, Semeling, 08100 Bedong, Malaysia

[6] Saveetha Dental College and Hospitals, Saveetha Institute of Medical and Technical Sciences, Chennai, Tamil Nadu, India